Journal of Alloys and Compounds, *176* (1991) 147–158
JAL 0008

Microstructure of AuCu II in the disordered f.c.c. phase of AuCu–14at.%Ag alloy

Koh-Ichi Udoh, Katsuhiro Yasuda, Gustaaf Van Tendeloo and Joseph Van Landuyt
Department of Dental Materials Science, Nagasaki University School of Dentistry, Nagasaki (Japan) and University of Antwerp (RUCA), Antwerp (Belgium)

(Received April 25, 1991)

Abstract

Microstructural changes related to AuCu ordering and two-phase decomposition were studied by means of conventional transmission electron microscopy and high resolution electron microscopy in an AuCu–14at.%Ag pseudobinary alloy. Two different types of precipitates, spindle type and chain type, are formed by a nucleation and growth process upon annealing at 643 K. These precipitates are termed "composite precipitates" because they show a sandwich structure consisting of blocks of a silver-rich f.c.c. phase (α_2) and AuCu II ordered thin platelets along two of their three faces. Only their lateral faces were not decorated and connected directly with the copper-rich α_1 matrix. By aging just below the spinodal line, the blocks of α_2 f.c.c. were completely sandwiched by the AuCu II ordered thin platelets. A model explaining these configurations is proposed. In the present alloy a modulated structure is also found by aging for short periods at low temperature.

1. Introduction

When silver is added to an equiatomic AuCu alloy, three distinguishable phase transformations may occur depending on the silver content and on the annealing temperature:

(a) AuCu I and/or AuCu II ordering from the disordered solid solution by a nucleation and growth mechanism (N–G process);

(b) ordering and two-phase decomposition promoted by the N–G process;

(c) ordering resulting from spinodal decomposition.

It is also observed that the ordering occurs at the grain boundaries by a discontinuous mechanism at a later stage of aging provided that the alloy is located inside the miscibility gap.

Since no exact phase diagram has been determined yet, particularly at the AuCu-rich side in the AuCu–Ag pseudobinary system, no concrete details on miscibility gap and ordering mechanisms are known. Because practical dental gold alloys are located in this composition region, it is of great importance to determine the details of this phase diagram.

Generally a lot of effort is needed to determine an equilibrium phase diagram of a ternary system and it requires a large amount of experimental

0925-8388/91/$3.50

work to investigate the alloy behaviour for different temperatures and compositions. Furthermore, in order to obtain equilibrium, long annealing times are required.

Previously a coherent phase diagram of the $Au_X(Ag_{0.24}Cu_{0.76})_{1-X}$ section of the Au–Cu–Ag ternary system was determined, mainly by electron microscopy [1]. This work was carried out on the basis of a hypothesis proposed by Allen and Cahn [2]. According to these authors, thermodynamic equilibrium need not be attained; they argue that the coherent phase must be in metastable equilibrium and must be unstable in the presence of the incoherent phases. It is therefore clear that the coherent phase diagram is also informative with respect to the age hardening associated with transformations.

For this systematic study on the coherent phase diagram of the AuCu–Ag section in the Au–Cu–Ag ternary system it is important to locate and identify the disordered f.c.c. phase coexisting with the AuCu ordered phase. In the AuCu–5.6at.%Ag alloy the silver-rich f.c.c. phase was present as finely dispersed precipitates, sometimes as small as 10 nm×2 nm, coexisting with AuCu I and/or AuCu II ordered phases depending on the aging temperature. These results were obtained by high resolution electron microscopy (HREM) and conventional transmission electron microscopy (TEM) [3]. Furthermore, a disordered f.c.c. solid solution which was predicted from the phase rule was also found adjacent to the tips of microtwin platelets when these are in contact with other orientation variants of the microtwin platelets. This is clearly the result of strain accommodation in AuCu–3at.%Ag alloy [4].

The present study is undertaken to clarify the coexistence of the AuCu I and/or AuCu II ordered and disordered f.c.c. phases and to examine the changes in structural configuration of these phases as a function of aging temperature in a AuCu–14at.%Ag pseudobinary alloy. From previous work it is known that in this alloy the spinodal locus is estimated at 640 K [5].

2. Experimental details

An ingot with composition Au–43at.%Cu–14at.%Ag as determined by chemical analysis was prepared by melting gold, copper and silver of better than 99.99% purity in a high frequency induction furnace. After homogenizing the ingot at 1073 K for several hours, a sheet of thickness 0.1 mm was obtained by cold rolling.

Discs 3 and 2.3 mm in diameter were punched out from the sheets and then sealed in evacuated tubes, annealed at 1073 K for 3.6 ks to establish the disordered solid solution and quenched in ice brine. The discs were then aged at 573, 623 and 643 K for various periods of time. They were electrothinned to transparency by a double-jet technique in a solution of 35 g of chromium trioxide in 200 ml of acetic acid and 10 ml of distilled water. Conventional 200 kV TEM observations were carried out using a side-entry electron microscope at Nagasaki University School of Dentistry, while HREM studies were performed at 200 and 400 kV with top-entry-type electron

microscopes at the Centre of Electron Microscopy for Materials Science of the University of Antwerp (RUCA).

3. Results and discussion

3.1. Precipitation upon aging at 643 K

Figure 1 shows a bright field TEM micrograph taken from a specimen aged at 643 K for 100 ks, *i.e.* within the temperature region where nucleation and growth processes are to be expected [5]. In the image, two different types of precipitates denoted A and B are observed along the ⟨100⟩ direction of an α_0 disordered matrix. The configuration of precipitate A resembles a chain, while precipitate B has a spindle-like shape; however, both precipitates partly contain ordered thin platelets, as will be shown next.

Figures 2(a)–2(c) show the same spindle-like precipitate under dark field conditions using the 110, 001 superlattice and $200\alpha_2$ fundamental reflections respectively. The configuration corresponds to aging at 643 K for 10 ks. A selected area electron diffraction (SAED) pattern over this precipitate is shown in Fig. 2(d). The diffraction pattern is indexed according to the f.c.c. α_0 disordered lattice. Because these precipitates no longer have cubic symmetry and since their c axes are roughly oriented along orthogonal directions of the matrix, it is impossible to obtain a SAED pattern perfectly oriented for

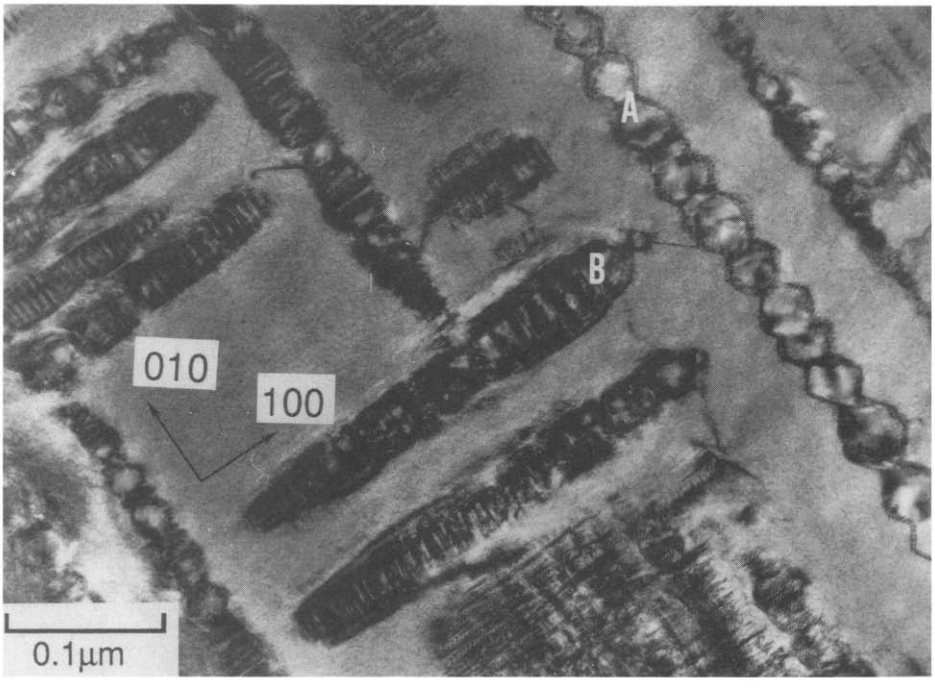

Fig. 1. Microstructure of an AuCu–14%Ag specimen aged at 643 K for 100 ks.

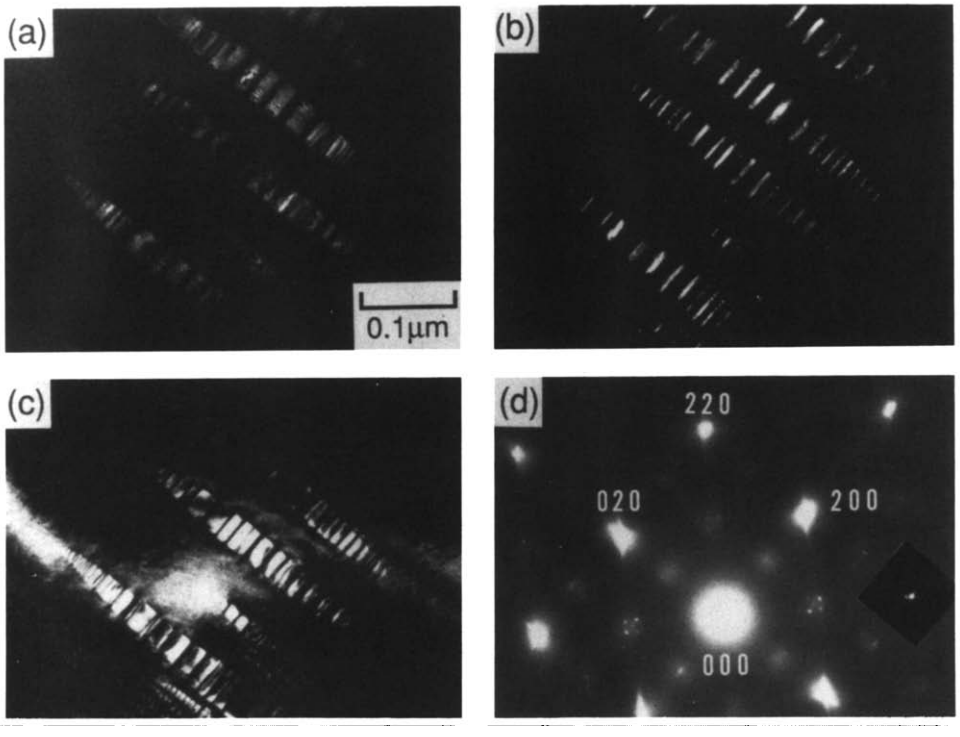

Fig. 2. TEM images and SAED pattern taken from a sample aged at 643 K for 10 ks: (a)–(c) dark field images using the 110, 001 superlattice and 220 fundamental reflections respectively; (d) corresponding SAED pattern.

all orientations. In Fig. 2(d) three orientation variants of the AuCu II ($L1_0$-S) ordering are clearly visible together with reflections from a long period antiphase domain boundary (LPAPB) structure which is also observed in Figs. 2(a) and 2(b). Furthermore, there is evidence for the precipitation of the α_2' phase, which is a metastable silver-rich f.c.c. phase; this is evident from the fine structure of the 220 reflection which is outlined. A comparison of Figs. 2(a) and 2(c) shows clearly that the AuCu II ordered thin platelets which have their c axis parallel to $[001]_{\alpha_0}$ (Z variant) are (in projection) superimposed on the α_2' phase. On the other hand, AuCu II platelets of another orientation variant with the c axis parallel to $[010]_{\alpha_0}$ (Y variant) are sandwiched between two α_2' blocks. Note that the $[100]_{\alpha_0}$ (X variant) orientation variant of AuCu II is never observed.

Thus the spindle-like precipitates are composed of AuCu II ordered platelets and α_2' phase blocks; they can be called "composite precipitates". The chain-like precipitate designated A in Fig. 1 also contains the Y variant of AuCu II between the two α_2' phase blocks which show a hexagonal or octagonal shape. These precipitates, however, are not surrounded by the Z variant of AuCu II.

A schematic model of the complex precipitate is shown in Fig. 3. It looks evident from our observations that the chain-type precipitate (A in Fig. 1) and the spindle-like precipitate (B in Fig. 1) actually have the same microstructure, but A is a view along the X direction while B is a view along the Z direction. Therefore there are three orientation variants of AuCu II present in the SAED pattern of Fig. 2(d) if the SAED pattern is taken from a region containing both types of composite precipitates. Figure 4 shows a three-dimensional picture of the atomic arrangement from the part of the

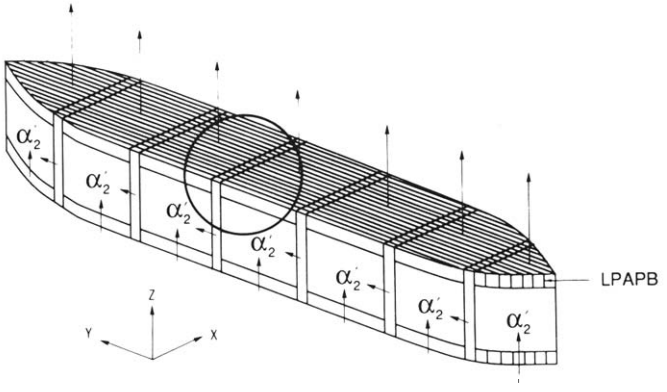

Fig. 3. Schematic representation of the spindle-like composite precipitate. The arrows indicate the direction of the c axis of the tetragonal $L1_{0\text{-}S}$ superlattice; "LPAPB" means a long period antiphase domain boundary.

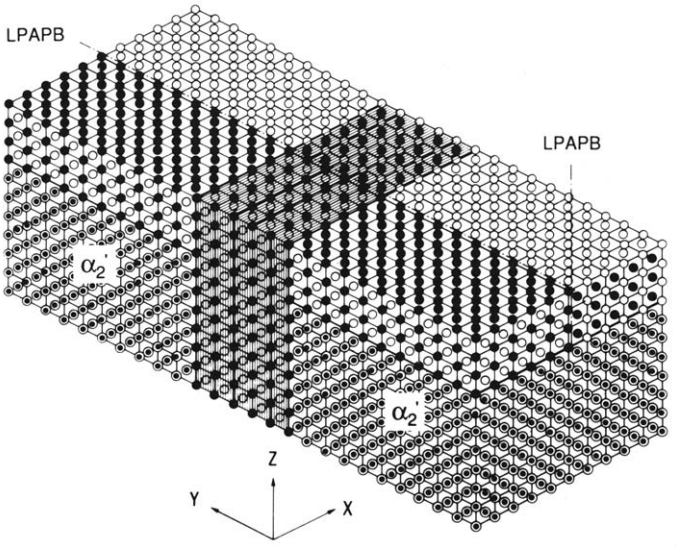

Fig. 4. Atomic-scale model of part of the composite precipitate enclosed by a circle in Fig. 3. Open circles represent gold atoms; filled circles are copper atoms; double circles show the silver-rich Ag–Cu solid solution, *i.e.* the α_2' f.c.c. phase. A different orientation variant of AuCu II is represented as a hatched region.

composite precipitate indicated by a circle in Fig. 3. A block-like α_2' phase is covered with an AuCu II platelet oriented along the Z direction and is intersected by an AuCu II platelet oriented along the Y direction. The long period is oriented perpendicular to the interface between the α_2' phase and the AuCu II platelets and runs continuously across both AuCu II variants (Y and Z). Following the longitudinal axis of the precipitate, it is clear that the dimensions of the Y variant of AuCu II become smaller at the tip than in the central part (see Fig. 2(b)). The average spacing is approximately 15 nm in the central part. These composite precipitates grow upon aging by selective growth along the longitudinal axis of the spindle or chain, but the growth rate is slow.

A different stage in the growth of the composite precipitate is shown in Fig. 5 after aging at 643 K for 100 ks. Figures 5(a)–5(c) are dark field images obtained by using the 110, 001 superlattice and $220\alpha_2$ fundamental reflections respectively. The SAED pattern is represented in Fig. 5(d). The LPAPB structure corresponding to the Z variant of AuCu II is clearly visible in Fig. 5(a). The spacing between Y variants is no longer uniform because of an irregular growth of the α_2' phase.

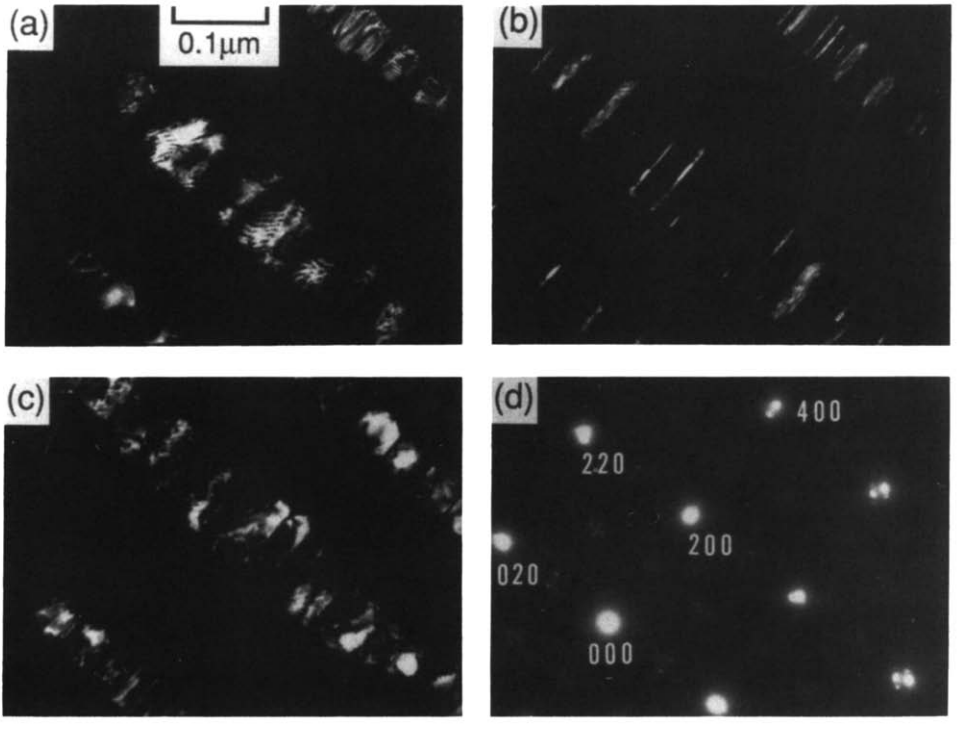

Fig. 5. TEM images and SAED pattern taken from a specimen aged at 643 K for 100ks: (a)–(c) dark field images using the 110, 001 superlattice and $220\alpha_2'$ fundamental reflection respectively; (d) corresponding SAED pattern.

3.2. Phases produced by aging at 623 K

Figures 6(a)–6(c) exhibit dark field images from a specimen aged at 623 K for 1 Ms produced by using the $220\alpha_2$ fundamental reflection, the $220_{\text{AuCu II},X,Y}$ fundamental reflection and the 110 superlattice reflection respectively. The SAED pattern corresponding to this area is shown in Fig. 6(d). It is verified that this pattern is indeed due to AuCu II and the α_2' phases; the 220 diffraction spot due to α_2' phase can be distinguished from the $200_{\text{AuCu II},Z}$ fundamental spot as seen in Fig. 6(d) and in its schematic representation of Fig. 7. The SAED pattern is a superposition of the α_2' f.c.c. phase and three orientation variants of the AuCu II ordered phase, *i.e.* *X*, *Y* and *Z* variants. The α_2' phase is identified as the cuboidal areas from Figs. 6(a) and 6(b), since they light up bright in (a) and remain dark in (b). These cuboidal α_2' blocks are completely surrounded by the AuCu II.

From the above observations the microstructural model of Fig. 8 is deduced. Thin platelets of the *Z* variant of AuCu II are sandwiched between cuboidal α_2' blocks. These α_2' blocks are enclosed all around by AuCu II; for clarity reasons, however, the top and bottom parts are not indicated. Therefore twin boundaries are found as eight slanting surfaces (prisms) at

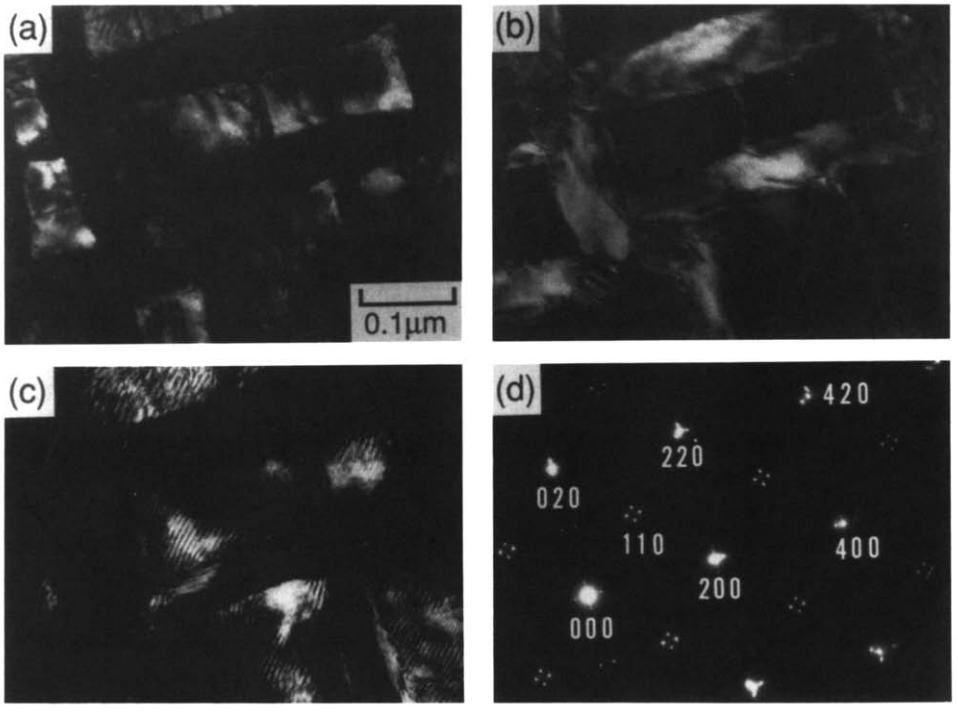

Fig. 6. TEM images and SAED pattern taken from a sample aged at 623 K for 1 Ms: (a)–(c) dark field images using the $220\alpha_2'$, $202_{\text{AuCu II},X,Y}$ fundamental and 110 superlattice reflections respectively; (d) corresponding SAED pattern.

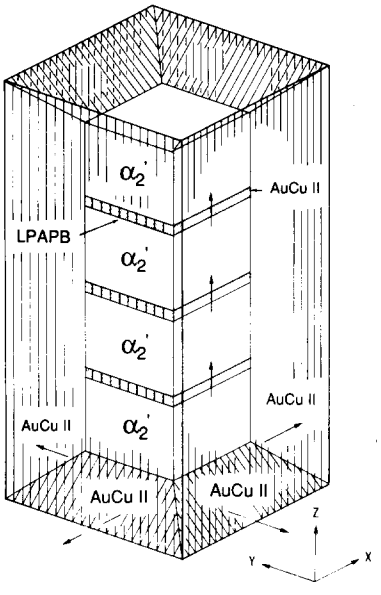

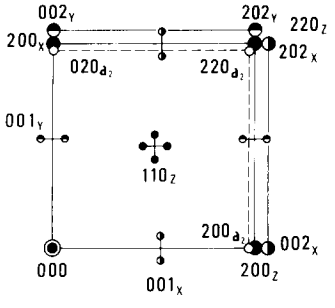

Fig. 7. Schematic representation of the SAED pattern of Fig. 6(d). The Miller indices used here refer to the $L1_0$ superlattice; the subindices refer to the different orientation variants.

Fig. 8. Possible structural configuration of the coexisting phases formed by aging at 623 K. The arrows indicate the orientation of the c axis of the AuCu II phase; parallel lines indicate the LPAPBs; the hatched areas indicate the AuCu II ordered platelets sandwiched between α_2' phase blocks.

the top and bottom parts in addition to four longitudinal prismatic planes originating from each corner of the α_2' block.

The above structural configuration is also suggested from the HREM micrograph of Fig. 9, which is taken from a specimen aged at 623 K for 100 ks. It can be seen that the cuboidal α_2' blocks are fully enclosed by the AuCu II phase. The LPAPBs are perpendicular to the interface between the α_2' block and AuCu II phase. An idealized atomic configuration of the above example is reproduced in Fig. 10. In order to surround the α_2' with the AuCu II phase, it is necessary that twinning is introduced to relieve the strain associated with the tetragonality of the ordered structure. In the case of Fig. 10 the SAED pattern would consist of a superposition of two diffraction patterns which are related to each other by a simple rotation of 2ϕ about the direct spot. The angle ϕ is the orientation difference between the original cube axis of the disordered f.c.c. phase and either the c or a axis of the tetragonal phase; it is defined by the formula $tan(\pi/4-\phi)=c/a$ [6]. However, such a rotation is not observed in the SAED pattern of Fig. 6(d), in spite of the expected c/a ratio of 0.93. Therefore it is assumed that the strain introduced by the tetragonality of the AuCu ordering is accommodated by the cuboidal α_2' blocks, *i.e.* the contraction of the AuCu II ordered thin platelets along the c axis is compensated by a mutual arrangement of the

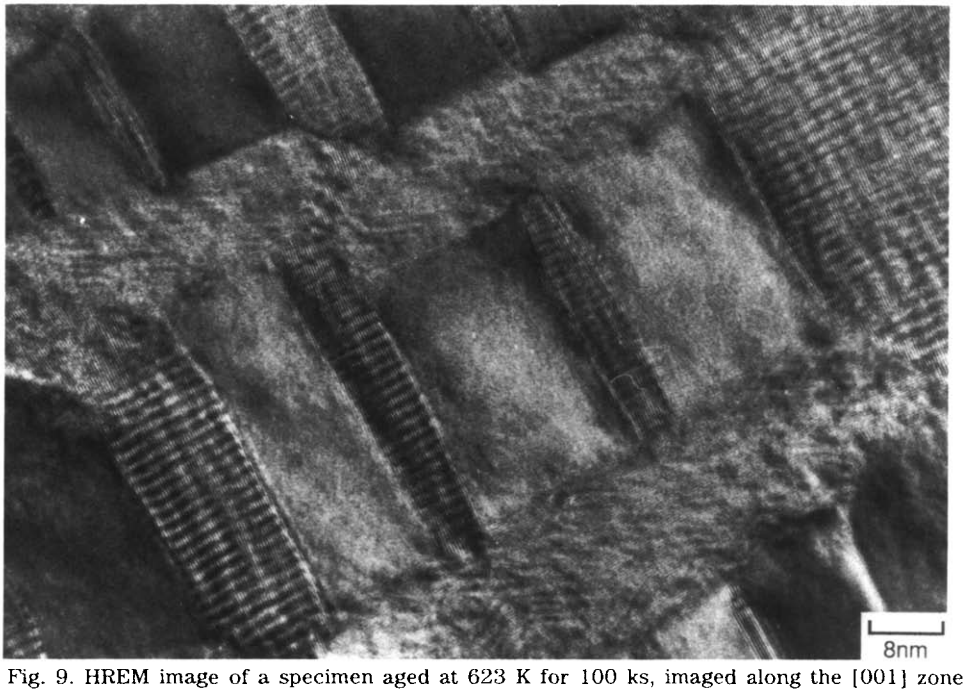

Fig. 9. HREM image of a specimen aged at 623 K for 100 ks, imaged along the [001] zone axis.

α_2' blocks. The expected lattice parameter of the α_2' phase is approximately 10% larger than the lattice spacing in the AuCu II platelets along this direction. In fact, strain contrast is visible just inside the α_2' blocks close to the interface. By inspection of Fig. 9 it is clear that the interface between the α_2' block and the Z variant of the AuCu II platelet is not a plane surface but a curved interface. This also plays an important role in accommodating the local strain introduced by ordering.

This structural configuration originates from a mechanism different from that for the composite precipitates which are formed by the N–G process, because the aging temperature of 623 K is just below the spinodal temperature of 640 K. Miyazaki *et al.* [7] treated theoretically the two-phase decomposition derived from the Fourier expression of the non-linear diffusion equation on the basis of the Cahn–Hilliard flux equation. They show that composition profiles of the solute appear as rectangular-shaped waves rather than modulated oscillatory waves as function of aging for an alloy with a composition just inside the spinodal locus. According to them, the α_2' blocks show a tendency towards the N–G process, even though the aging temperature is just below the spinodal temperature.

3.3. Two-phase decomposition and ordering at 573 K

Figure 11(a) and 11(b) show an HREM micrograph and an SAED pattern respectively from a specimen aged at 573 K for a short period of 30 s. The

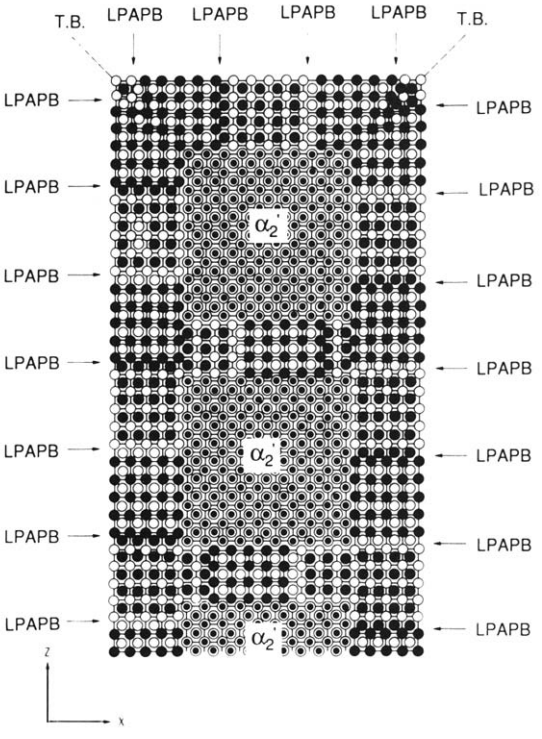

Fig. 10. Atomic-scale representation of the HREM image shown in Fig. 9. Open circles are gold atoms; solid circles are copper atoms; double circles indicate the α_2' silver-rich f.c.c. phase; "T.B." locates the twin boundaries.

HREM micrograph shows a crystallographic anisotropy of the microstructure which has a periodicity in solute distribution, *i.e.* a modulated structure. This microstructure consists of several different microdomains only one or a few nanometres wide; some of these are indicated in Fig. 11(a) as A, B, C and D. In the areas A and B the white (or dark) lines, separated by 0.4 nm, clearly indicate a doubling of the cubic (002) periodicity and the structure can be identified as AuCu I. The direction of the *c* axis of these f.c.t. ordered areas lies in the plane and is indicated by arrows. The area C on the other hand is also AuCu I ordered but its *c* axis is perpendicular to the image. This identification is compatible with the SAED pattern shown in Fig. 11(b), in which only very weak superlattice reflections at 100, 010 and 110 are present.

Apart from these ordered domains, silver-rich f.c.c. areas (denoted D in Fig. 11(a)) are also present in this microdomain structure; this can be concluded from the local spacing as well as from the SAED pattern of Fig. 11(b), where diffuse sidebands are present at the basic reflections along the ⟨100⟩ directions. This spinodal-decomposition-type behaviour indicates a periodic composition fluctuation along ⟨100⟩. Even if AuCu ordering is superimposed on the spinodal decomposition, one can distinguish the effect

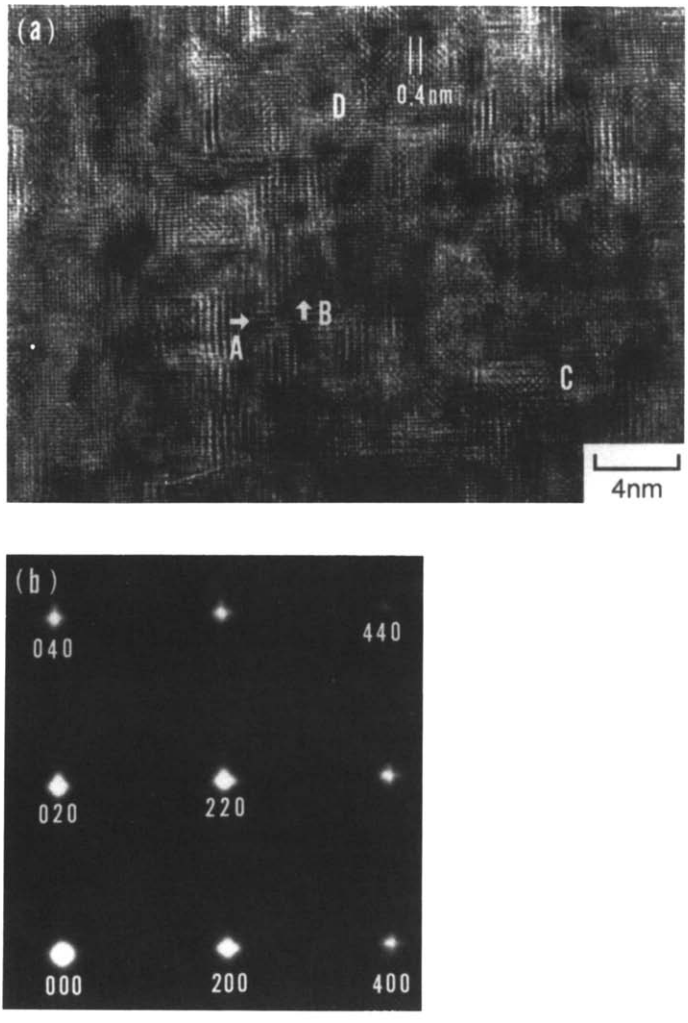

Fig. 11. (a) HREM image and (b) corresponding SAED pattern of a specimen aged at 573 K for 30 s. A, B and C indicate microdomains of three different orientation variants of the AuCu I structure; D is an f.c.c. microarea. Arrows mark the direction of the *c* axis.

on the diffraction pattern. When AuCu I ordering (in three variants) occurs, the 200 and equivalent fundamental reflections are elongated away from the direct spot (origin); the presence of silver-rich f.c.c. microdomains, however, will produce a spot elongation towards the origin, since their lattice parameter is larger than that of the AuCu I superlattice. In Fig. 11(b) both effects are clearly present; it is therefore concluded that spinodal decomposition occurs in association with AuCu I ordering in the early stages of ordering at 573 K.

Acknowledgment

The authors gratefully acknowledge the financial support of the present work by the Japanese Ministry of Education, Science and Culture through Grant 01044112 under the Monbusho International Scientific Research Program (Joint-Research).

References

1 M. Nakagawa and K. Yasuda, *J. Less-Common Met.*, *138* (1988) 95.
2 S. M. Allen and J. W. Cahn, *Acta Metall.*, *23* (1975) 1017.
3 K. Yasuda, M. Nakagawa, G. Van Tendeloo and S. Amelinckx, *J. Less-Common Met.*, *135* (1987) 169.
4 K. Yasuda, M. Nakagawa, K. Udoh, G. Van Tendeloo and J. Van Landuyt, *J. Less-Common Met.*, *158* (1990) 301.
5 K. Hisatsune, K. Udoh, B. I. Sosrosoedirdjo, T. Tani and K. Yasuda, *J. Alloys Comp.*, in the press.
6 S. Yamaguchi, *Jpn. J. Appl. Phys.*, *5* (1966) 496.
7 T. Miyazaki, T. Kozakai, S. Mizuno and M. Doi, *Trans. Jpn. Inst. Met.*, *24* (1983) 246.